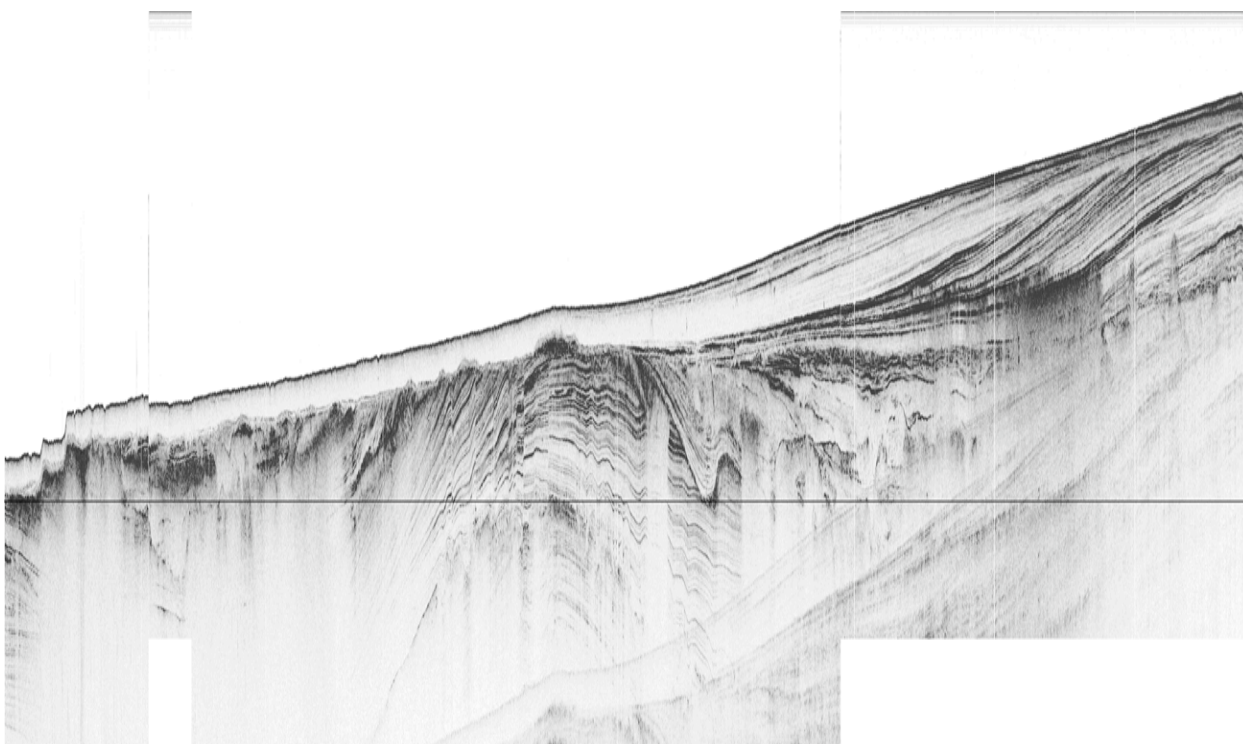


Cruise Report MV220402: Clinoform Sequence Stratigraphy in a Modern Foreland

Co-Chief Scientists:

**John Milliman
Neal Driscoll**



Cruise Participants

Cruise Participants MV220402

Jeff Babcock – Project Scientist, Scripps Institution of Oceanography, University of California, San Diego

Neal Driscoll – Professor, Scripps Institution of Oceanography, University of California, San Diego

Denise Elwood – Scripps Institution of Oceanography, University of California, San Diego volunteer

Rebecca Fenwick – Graduate Student, Scripps Institution of Oceanography, University of California, San Diego

Jenna Hill – Graduate Student, Scripps Institution of Oceanography, University of California, San Diego

John Milliman – Professor, College of William & Mary

Matt Niemitz – JOI Fellowship

Rudy Slingerland – Professor, Penn State University

John Walsh – Assistant Professor, East Carolina University

Preliminary Shipboard Results MV220402: Clinoform Sequence Stratigraphy in a Modern Foreland

Neal Driscoll, John Milliman, Rudy Slingerland, J. P. Walsh, Jeffrey Babcock

The MARGINS Source to Sink program in the Papua New Guinea foreland basin is providing a unique opportunity to determine the genesis and character of foreland stratigraphic sequences as a function of ice-house eustatic sea-level fluctuations, high sediment fluxes, and foreland-style tectonic subsidence.

Although our team is collecting data aboard the R/V Melville as we write this, we already have identified an apparent relationship between relative sea-level change and the genesis of the Gulf of Papua clinoform sequences. Preliminary analysis of 21 piston cores, 24 gravity cores, 1300 nmi of deep-towed CHIRP and more than 2500 nmi of hull-mounted CHIRP sub-bottom profiles in the southern Papua New Guinea foreland basin shows that this shelf is characterized by two distinct stratigraphic units: 1) a modern clinoform on the inner shelf thickening to the north and west whose topsets lie at approximately 20 m water depth and whose foresets extend down to 50-70 m, and 2) an older, as yet un-dated thick sequence of horizontal strata that underlies at least the lower portion of the foresets and extends seaward across the middle shelf (Fig. 1). We interpret this unit as an older clinoform. This unit has been dissected into cross-shelf trending channels separated by elongate topographic highs as first noted by Harris et al. (1996). The little modern sediment that mantles this eroded landscape lies mostly in the topographic lows.

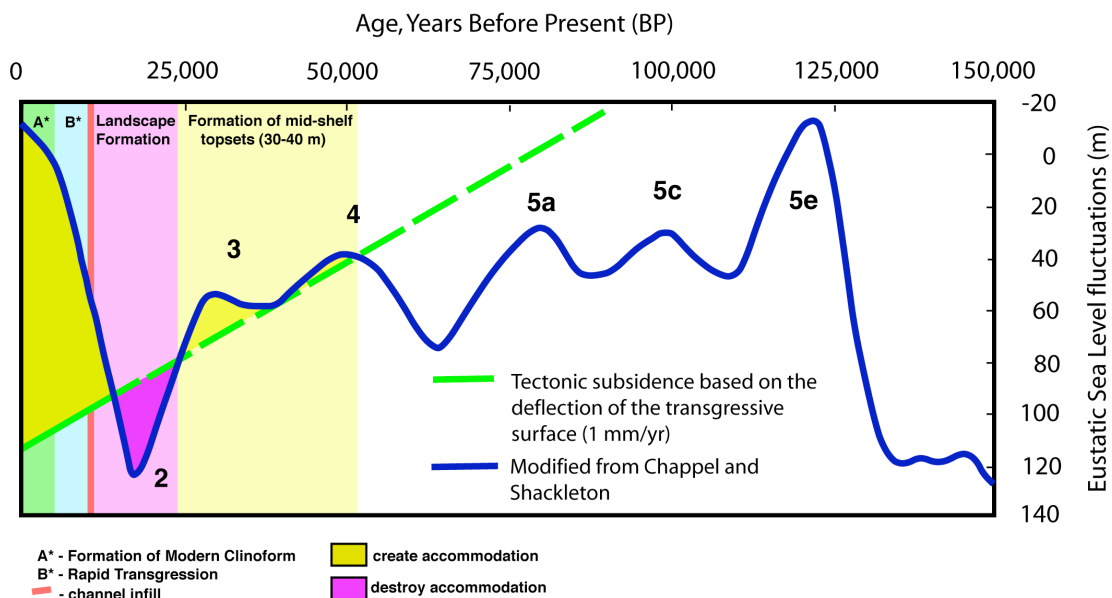


Figure 1. Conceptual sea level subsidence model illustrating clinoform development, erosion and redevelopment in the Gulf of Papua

Based on the configuration of the horizontal strata within the middle shelf clinoform, their stiff character when cored, and their present elevation, we deduce that the mid-shelf clinoform prograded two-thirds of the way across the pre-existing shelf in response to relative sea-level rise during stage 3 and possibly stage 4, when the rate of tectonic subsidence outpaced the rate of eustatic sea-level fall; the resulting newly created accommodation was roughly equal to the sediment input from the Fly, Kikori, Purari, and other coastal rivers. These may be the first stage-3 clinoforms reported from a continental shelf; topsets are 30-40 m thick. Deflection of the transgressive surface from horizontal yields a post-LGM differential subsidence of about 1 mm/yr from the peripheral bulge in the southwest to near the basin depocenter in the northeast. On the basis of the Chappel and Shackleton eustatic sea level curve, eustatic sea level fell from ~-40 to ~-80 m between 45,000 and 25,000 years BP. During this period, tectonic subsidence must have outpaced eustasy to create the observed 30-40 m of accommodation.

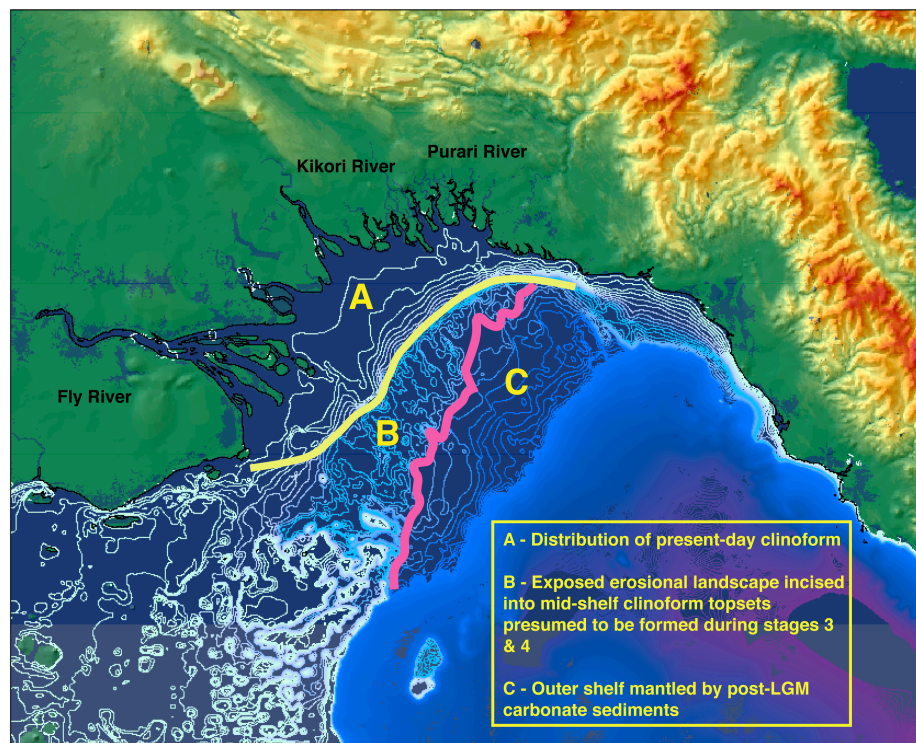


Figure 2. Gulf of Papua showing distribution of different morphologic provinces.

Without firm dates, however, we cannot negate the possibility that the topsets predate

stages 3 and 4, which thereby would require lower rates of tectonic subsidence to create the observed accommodation. Cut and filled channels within the topset sequence suggest short-term fluctuations in relative sea level, consistent with the Chappel and Shackleton sea-level curve.

The advent of Stage 2 resulted in a rapid eustatic fall commencing ~25,000 years BP that lowered sea level to -120 m, causing incision and headward erosion of streams across the topsets and seaward foresets. The consequent erosion created a

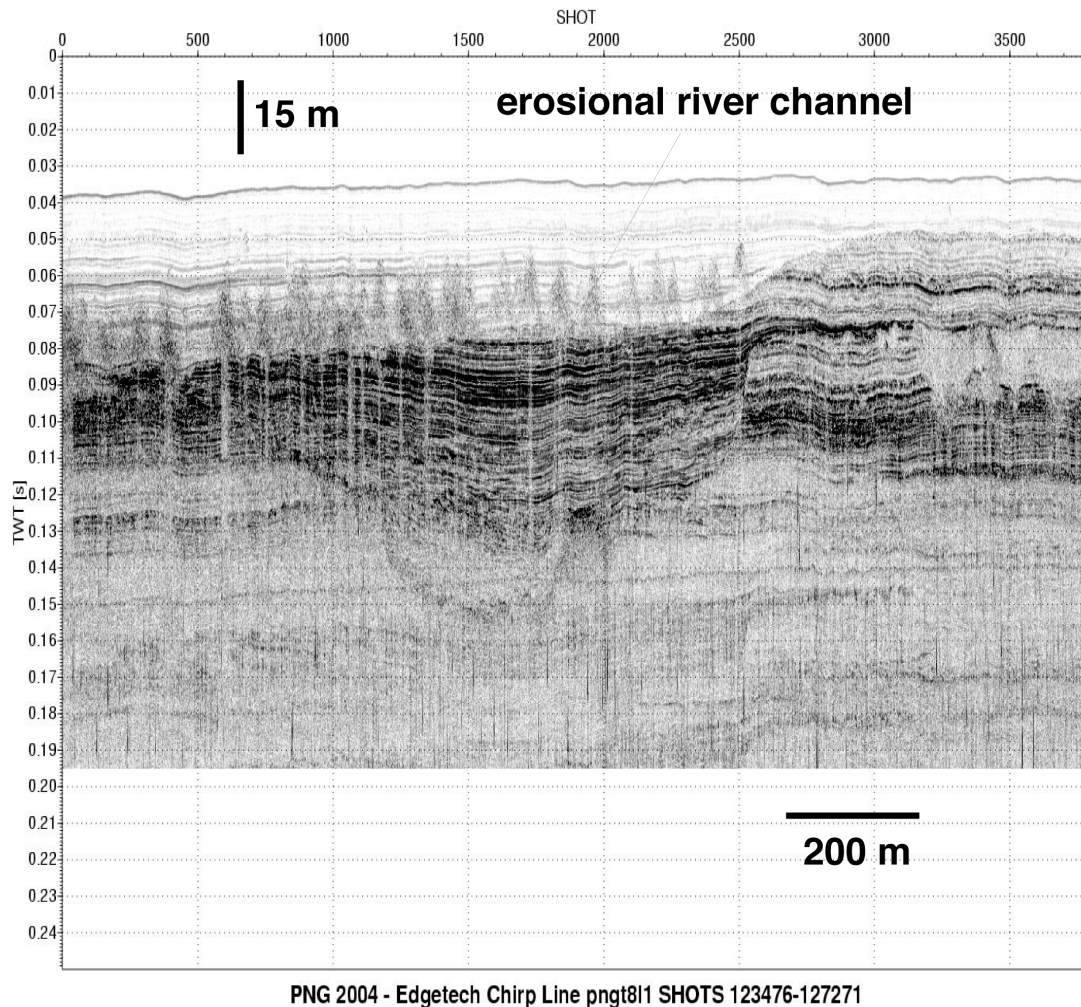


Figure 3. Chirp seismic line collected during our cruise MV220402 imaging the buried erosional landscape along the inner continental shelf

landscape with ~20-40 m of relief and a dendritic drainage pattern. As eustatic sea level rose from -120 to +3 m about 7,000 years BP, the former mid-shelf river channels within the river valley were partially filled, presumably by fluvial and estuarine facies. The transgression was so rapid, however, that the valleys themselves remained unfilled except for minimal input from eroding interfluvies. During this rise the river mouths

backstepped landward, carbonate sediments began to be deposited on the outer shelf, blanketing the former alluvial plain. By 7,000 years BP the shoreline had migrated northwestward of its present position, although the precise location remains unknown. Sediment was sequestered close to shore, thereby preserving the drowned landscape that incised into the mid-shelf clinoform. From 7,000 years BP to present, sediment supply to the shelf exceeded the creation of new accommodation and the modern clinoform prograded seaward to its present position, progressively covering up the drowned landscape of the subjacent clinoform.

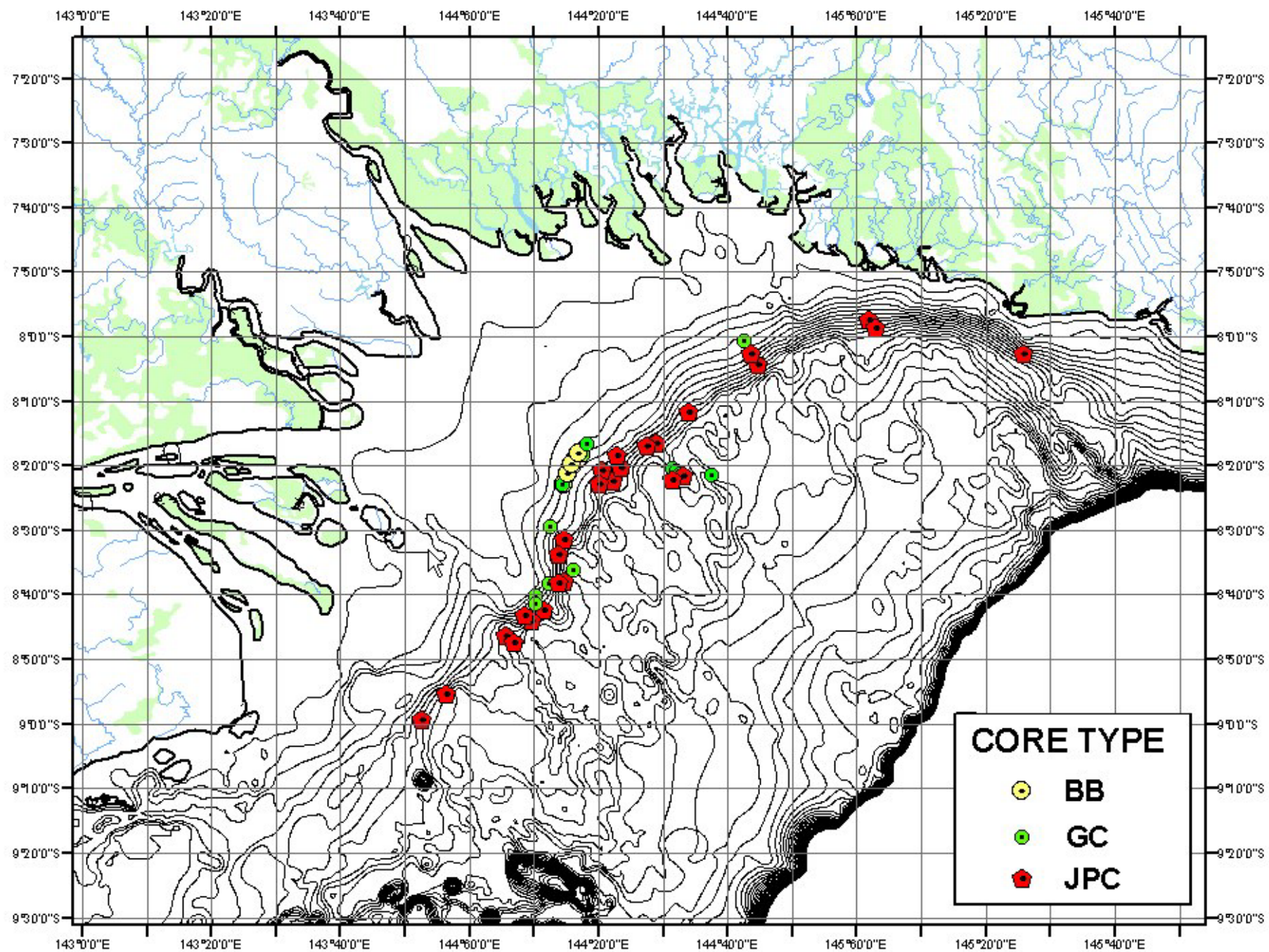
Our seismic profiles also provide evidence for the sediment transport processes that are building the modern clinoform. Much of the upper foreset sequence is composed of discrete sand/mud bars or lobes, which show a preponderance of northeast-dipping reflectors. These lobes appear to coalesce down the clinoform, presumably the result of downslope gravitational movement and along-slope smoothing by NE-flowing regional currents. Numerical modeling of circulation and sediment transport for the proposed paleogeographic configurations will help to test these ideas as will more detailed analysis of our piston and gravity cores co-registered with CHIRP profiles.

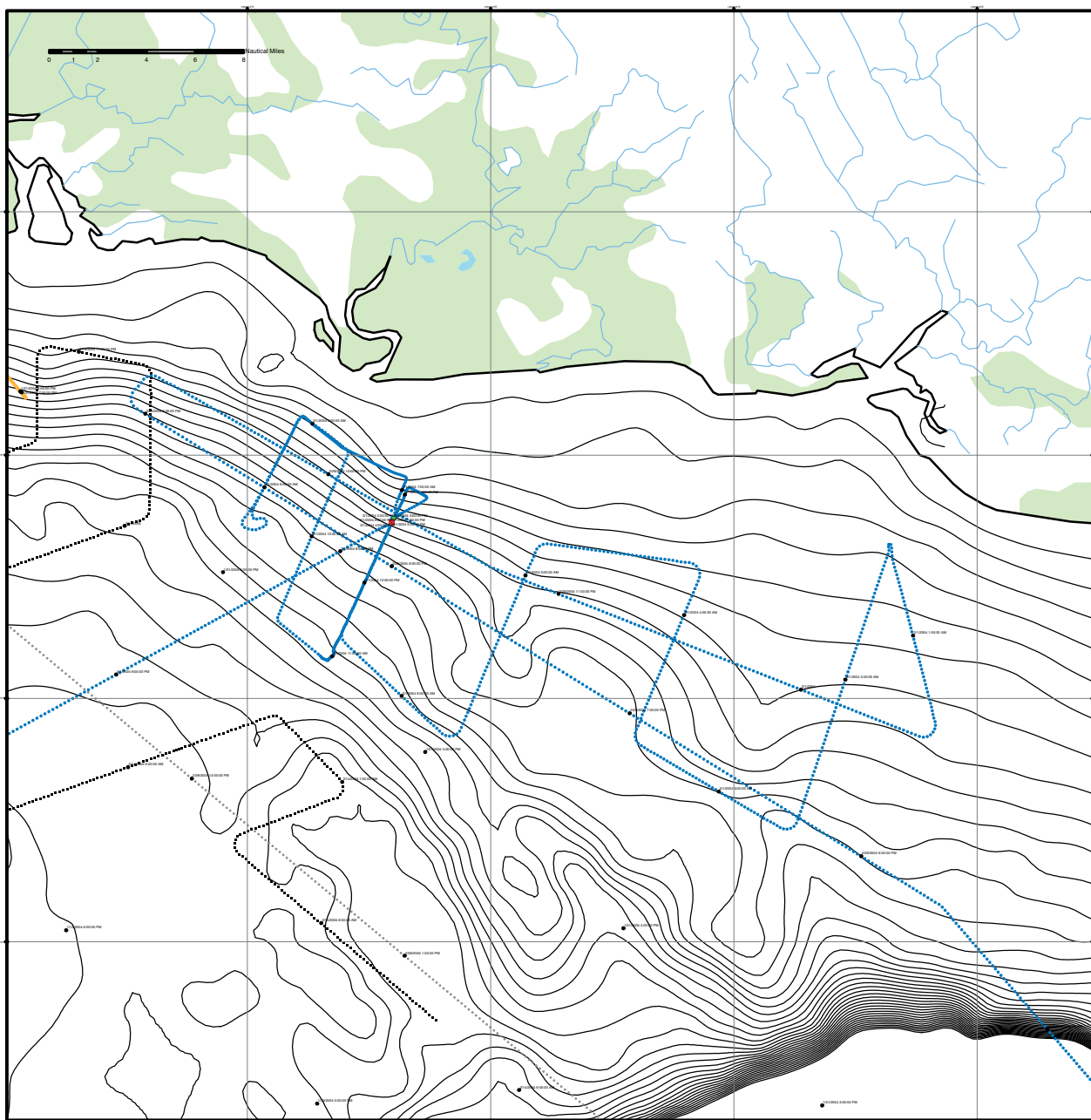
These preliminary observations suggest that tectonic subsidence typical of foreland basins can generate accommodation during ice-house eustatic sea-level falls. The asymmetry of ice-house sea-level fluctuations means that regressions average about 1 mm per year whereas transgressions can be an order of magnitude faster. Analysis of the sediment cores and dating of selected samples should provide evidence to support or modify this conceptual model.

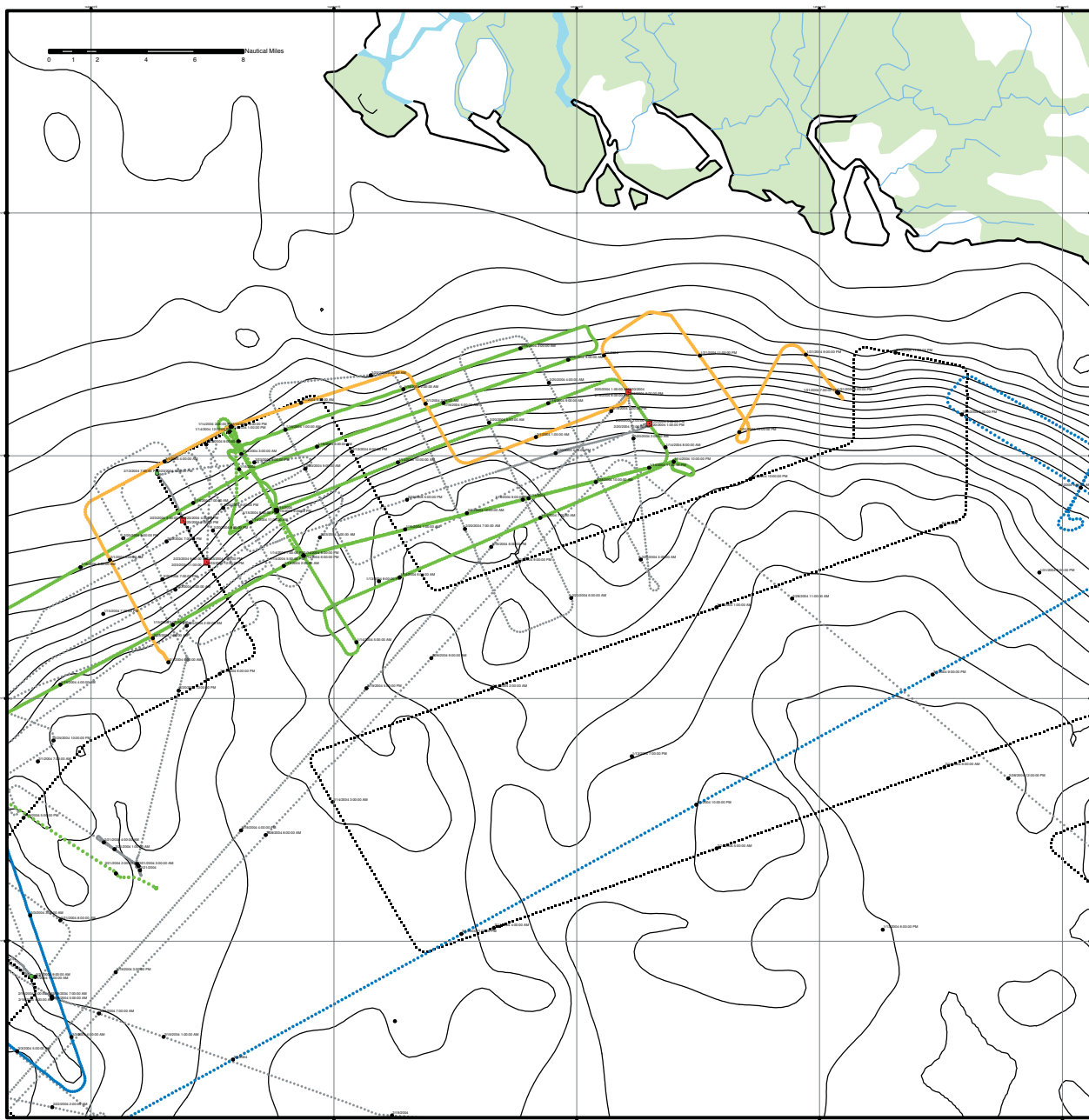
References

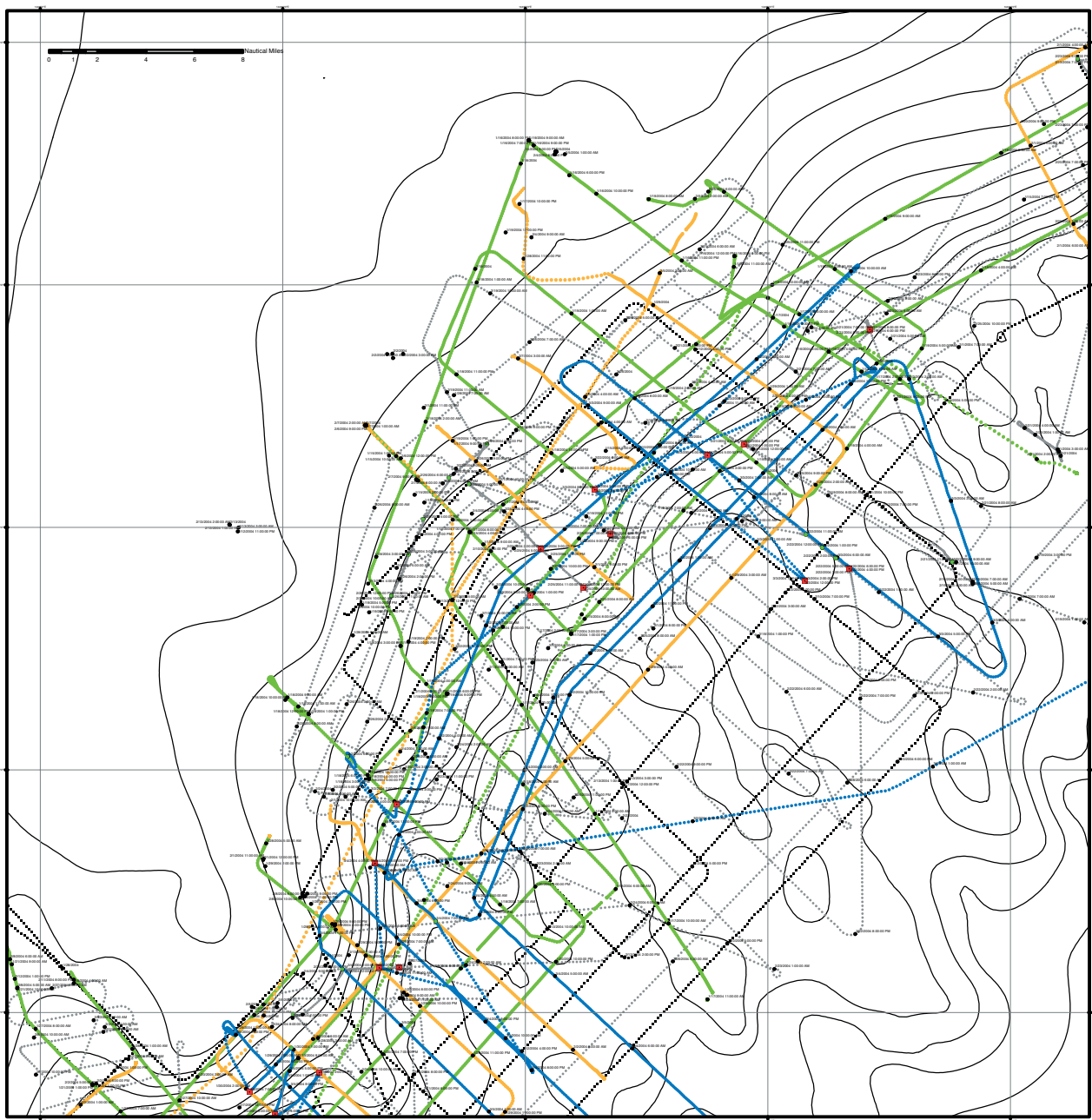
- Harris, P. T., C. B. Pattiaratchi, J. B. Keene, R. W. Dalrymple, J. V. Gardner, E. K. Baker, A. R. Cole, D. Mitchell, P. Gibbs, and W. W. Schroeder, 1996, Late Quaternary deltaic and carbonate sedimentation in the Gulf of Papua foreland basin: Response to sealevel change. *Journal of Sedimentary Research*, 66:801-819.

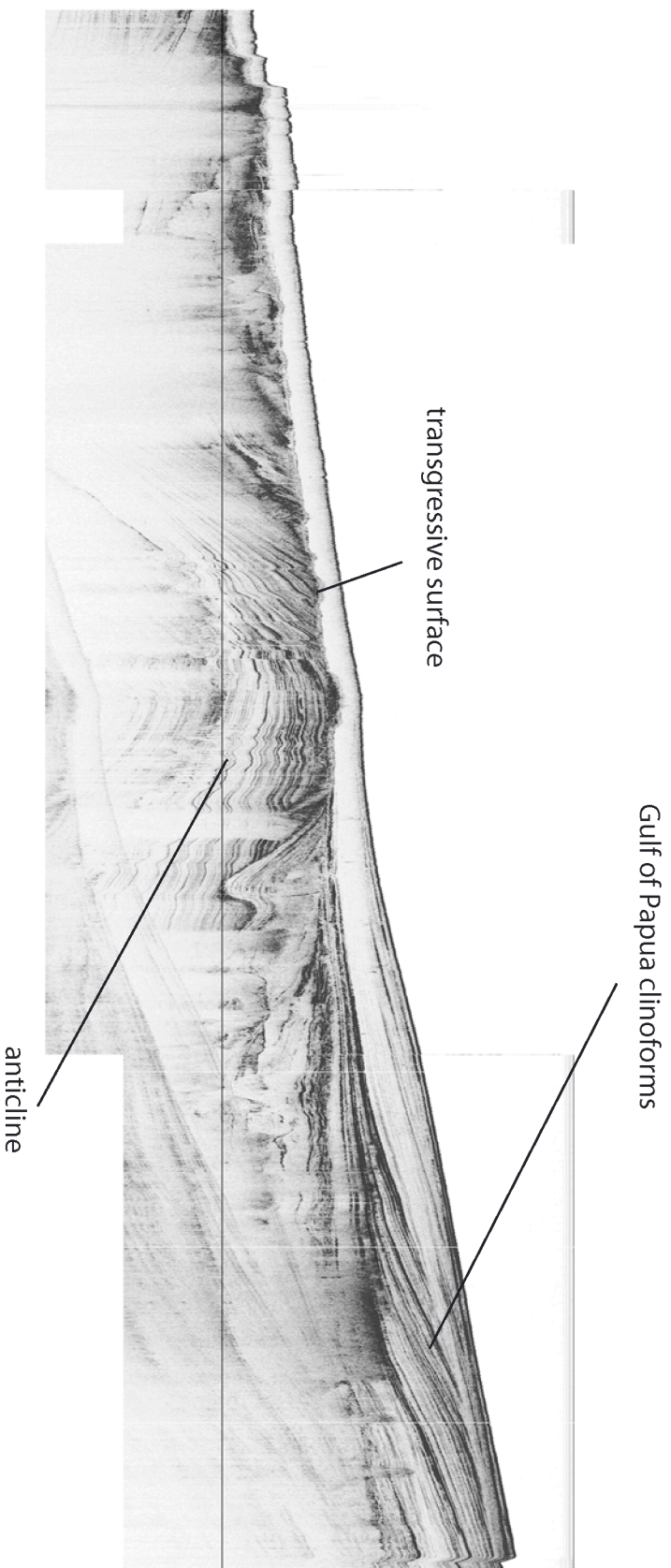
rv	crs	log date	station #	core ID	observer	lat d launch	lat m launch	lat d bott	lat m bott	long d launch	long m launch	long d bott	long m bott	nav type	sample type	t launch	t bott	t recov	d launch of bott	d recov	w launch	w bott	w recov	scope	trigger	pin	act d	d plinger	tension surf	tension trip	tension bott	tension max	tension asc	core length	TC type	remarks
Mahle MV22-0402	1	22054 0.00	1	1JC01	jenia H8	-7.656483	0	-7.656445	0	145.526283	145.526238	0	0	3	2	10000.020	10000.04	10000.033	53.9	53.9	54	-8	40	20	34	35				970	8000	4027	12456	9500	50	there is no PC section I-miscalculation on 30' core, this section ended up being chopped off.
Mahle MV22-0402	1	22054 0.00	2	2JC02	jenia H8	-7.67868	0	-7.678683	0	145.048977	145.048977	0	0	3	2	10000.1248	10000.1256	10000.133	62.2	62.8	62	0	45	24	24	48					8800	4700	17390	10000	40	void in core, top sec II - 12m at sec II bot bot sec IV - 4 cm
Mahle MV22-0402	1	22104 0.00	3	3JC03	jenia H8	-8.307187	0	-8.307187	0	144.630287	144.630287	0	0	3	4	10000.020	10000.025	10000.130	75	75	75	7	72	0							850	325	1100	700	10	7 lead weights +500m core
Mahle mv22-0402	1	22104 0.00	4	4JC04	dale Hubbard	-8.35707	0		0	144.63023		0	0	3	4	10000.1017	10000.1034		75.6												300	300	1423	860	10	replicate core from str 3, for PMG fakes. 9 lead wts on stand; wt = approx 625 lbs
Mahle mv22-0402	1	22104 0.00	5	5JC05	jenia H8	-8.376163	0	-8.376163	0	144.630283	144.630283	0	0	4	2	10000.1418	10000.1424	10000.1505	54.8	54.8	55	0	37	0	22	43					8000	6200	14700	11600	40	no section info
Mahle mv22-0402	1	22104 0.00	6	6JC06	jenia H8	-8.376933	0	-8.376933	0	144.609467	144.609467	0	0	4	2	10000.1832	10000.1838		52.2	55.1	55	0	37	0	22	48					9000	6000	14200	9500	40	12 lead weights + 750 lbs. Tension on bottom questionable.
Mahle mv22-0402	1	22204 0.00	7	7JC07	jenia H8	-8.338193	0	-8.338193	0	144.538193	144.538193	0	0	4	4	10000.1037	10000.1100	10000.2100	64.9	64.9	65	0	64	0							1000	154	1400	1000	10	same location as p07
Mahle mv22-0402	1	22204 0.00	8	8JC08	jenia H8	-8.338217	0	-8.338217	0	144.537775	144.537775	0	0	4	4	10000.1120	10000.1122	10000.1127	63.2	63.2	62	0	64	0							1000	150	1880	1000	10	
Mahle mv22-0402	1	22204 0.00	9	9JC09	jenia H8	-8.3472263	0	-8.3472263	0	144.537667	144.537667	0	0	4	4	10000.1212	10000.1222	10000.1230	69.4	69.7	69.7	5	70	0							1000	160			10	
Mahle mv22-0402	1	22204 0.00	10	10JC10	jenia H8	-8.3472217	0	-8.3472217	0	144.53766	144.53766	0	0	4	4	10000.1241	10000.1244	10000.1242	69.4	69.4	69.4	5	71	0							1000	180	1700	1000	10	
Mahle mv22-0402	1	22204 0.00	11	11JC11	jenia H8	-8.354467	0	-8.354467	0	144.54613	144.54613	0	0	4	4	10000.1330	10000.1333	10000.1340	67.1	67.1	67.1	5	73	0							1000	180			10	
Mahle mv22-0402	1	22204 0.00	12	12JC12	jenia H8	-8.36408	0	-8.36408	0	144.546273	144.546273	0	0	4	4	10000.1335	10000.1338	10000.1405	67.1	67.1	67.1	5	74	0							1000	200	1700	1200	10	
Mahle mv22-0402	1	22204 0.00	13	13JC13	jenia H8	-8.361975	0	-8.361975	0	144.556543	144.556543	0	0	2	2	10000.1638	10000.1633		82.6	82.6	82.6	0	65	0	22	48					9000	4700		10000	40	void sec II 72.5 cm sec II IV 216.5 cm void inside of X, at least 40 cm lower part of X got bagged
Mahle mv22-0402	1	22204 0.00	14	14JC14	jenia H8	-8.372883	0	-8.372883	0	144.56444	144.56444	0	0	2	2	10000.1638	10000.1633		82.6	82.6	82.6	0	65	0	22	48					9000	4800		10000	40	
Mahle mv22-0402	1	22204 0.00	15	15JC15	jenia H8	-8.372817	0	-8.372817	0	144.56442	144.56442	0	0	2	2	10000.1638	10000.1633		82.6	82.6	82.6	0	65	0	22	48					9000	4800		10000	40	
Mahle mv22-0402	1	22204 0.00	16	16JC16	jenia H8	-8.37146	-8	-8.37146	-8	144.56442	144.56442	0	0	2	2	10000.1638	10000.1633		82.6	82.6	82.6	0	65	0	22	48					9000	4800		10000	40	
Mahle mv22-0402	1	22204 0.00	17	17JC17	J.P. Walsh	-38.5088	-8	-38.5088	-8	144.80032	144.80032	0	0	2	2	10000.1317	10000.1323	10000.1354	58.6	58.2	58.6	-3	41	5	22	48					9008	6800	16700	9501	40	Void Sections 2 & 3 upper 62 cm of section 2 lower 39 cm of section 3
Mahle mv22-0402	1	22204 0.00	18	18JC18	jenia H8	-38.5098	-8	-38.5098	-8	144.80032	144.80032	0	0	2	2	10000.1317	10000.1323	10000.1354	58.6	58.2	58.6	-3	41	5	22	48					9008	6800	16700	9501	40	
Mahle mv22-0402	1	22204 0.00	19	19JC19	J.P. Walsh	-38.518	-8	-38.518	-8	144.80032	144.80032	0	0	2	2	10000.1317	10000.1323	10000.1354	58.6	58.2	58.6	-3	41	5	22	48					9008	6800	16700	9501	40	
Mahle mv22-0402	1	22204 0.00	20	20JC20	J.P. Walsh	-40.0228	144	-40.0228	144	10.43	10.43	144	10.43	4	4	10000.1633	10000.1634	10000.1637	23.2	23.2	23.2	0	31	0							1000	180	1540	1115	10	
Mahle mv22-0402	1	22204 0.00	21	21JC21	J.P. Walsh	-22.4818	144	-22.4818	144	22.387	22.387	144	22.387	4	4	10000.1633	10000.1634	10000.1637	23.2	23.2	23.2	0	31	0							1000	180	1540	1115	10	
Mahle mv22-0402	1	22204 0.00	22	22JC22	jenia H8	-20.862	144	-20.862	144	20.8204	20.8204	144	20.8204	4	4	10000.1633	10000.1634	10000.1637	23.2	23.2	23.2	0	31	0							1000	180	1540	1115	10	
Mahle mv22-0402	1	22204 0.00	23	23JC23	jenia H8	-18.2151	144	-18.2151	144	17.8857	17.8857	144	17.8857	4	4	10000.1633	10000.1634	10000.1637	23.2	23.2	23.2	0	31	0							1000	180	1540	1115	10	
Mahle mv22-0402	1	22204 0.00	24	24JC24	jenia H8	-20.862	144	-20.862	144	20.8204	20.8204	144	20.8204	4	4	10000.1633	10000.1634	10000.1637	23.2	23.2	23.2	0	31	0							1000	180	1540	1115	10	
Mahle mv22-0402	1	22204 0.00	25	25JC25	jenia H8	-22.8149	144	-22.8149	144	14.4808	14.4808	144	14.4808	4	4	10000.1633	10000.1634	10000.1637	23.2	23.2	23.2	0	31	0							1000	180	1540	1115	10	
Mahle mv22-0402	1	22204 0.00	26	26JC26	jenia H8	-22.8149	144	-22.8149	144	14.4808	14.4808	144	14.4808	4	4	10000.1633	10000.1634	10000.1637	23.2	23.2	23.2	0	31	0							1000	180	1540	1115	10	
Mahle mv22-0402	1	22204 0.00	27	27JC27	jenia H8	-22.8149	144	-22.8149	144	14.4808	14.4808	144	14.4808	4	4	10000.1633	10000.1634	10000.1637	23.2	23.2	23.2	0	31	0							1000	180	1540	1115	10	
Mahle mv22-0402	1	22204 0.00	28	28JC28	jenia H8	-21.7541	144	-21.7541	144	15.1302	15.1302	144	15.1302	4	4	10000.1633	10000.1634	10000.1637	23.2	23.2	23.2	0	31	0							1000	180	1540	1115	10	
Mahle mv22-0402	1	22204 0.00	29	29JC29	jenia H8	-19.8623	144	-19.8623	144	15.7974	15.7974	144	15.7974	4	4	10000.1633	10000.1634	10000.1637	23.2	23.2	23.2	0	31	0							1000	180	1540	1115	10	
Mahle mv22-0402	1	22204 0.00	30	30JC30	jenia H8	-17.9574	144	-17.9574	144	16.8539	16.8539	144	16.8539	4	4	10000.1633	10000.1634	10000.1637	23.2	23.2	23.2	0	31	0							1000	180	1540	1115	10	
Mahle mv22-0402	1	22204 0.00	31	31JC31	jenia H8	-16.5565	144	-16.5565	144	18.4167	18.4167	144	18.4167	4	4	10000.1633	10000.1634	10000.1637	23.2	23.2	23.2	0	31	0							1000	180	1540	1115	10	
Mahle mv22-0402	1	22204 0.00	32	32JC32	jenia H8	-16.5565	144	-16.5565	144	18.4167	18.4167	144	18.4167	4	4	10000.1633	10000.1634	10000.1637	23.2	23.2	23.2	0	31	0							1000	180	1540	1115	10	
Mahle mv22-0402	1	22204 0.00	33	33JC33	jenia H8	-46.4642	-8	-46.4642	-8	144.8469	144.8469	0	0	2	2	10000.1318	10000.1335	10000.1349	52.8	52.9	52.9	0	35	0	22	58					10000	4700	23500	13000	50	skipped-mislabelled
Mahle mv22-0402	1	22204 0.00	34	34JC34	jenia H8	-47.5013	-8	-47.5013	-8	144.8469	144.8469	0	0	2	2	10000.1318	10000.1335	10000.1349	52.8	52.9	52.9	0	35	0	22	58					10000	4700	23500	13000	50	40' of mud on outside of core barrel JPC cumulative lengths are base-wards (i.e. from bottom-to-top rather than from top-to-bottom)
Mahle mv22-0402	1	22204 0.00	35	35JC35	jenia H8	-47.5013	-8	-47.5013	-8	144.8469	144.8469	0	0	2	2	10000.1318	10000.1335	10000.1349	52.8	52.9	52.9	0	35	0	22	58					10000	4700	23500	13000	50	40' of mud on outside of core barrel JPC cumulative lengths are base-wards (i.e. from bottom-to-top rather than from top-to-bottom)
Mahle mv22-0402	1	22204 0.00	36	36JC36	jenia H8	-47.5013	-8	-47.5013	-8	144.8469	144.8469	0	0	2	2	10000.1318	10000.1335	10000.1349	52.8	52.9	52.9	0	35	0	22	58					10000	4700	23500	13000	50	40' of mud on outside of core barrel JPC cumulative lengths are base-wards (i.e. from bottom-to-top rather than from top-to-bottom)
Mahle mv22-0402	1	22204 0.00	37	37JC37	jenia H8	-2.8884	145	-2.8884	145	26.9463	26.9463	145	26.9463	4	4	10000.1633	10000.1634	10000.1637	23.2	23.2	23.2	0	31	0							1000	180	1540	1115	10	











Chirp seismic profile across the Northern Gulf of Papua illustrating clinoform development along the margin. The Gulf of Papua is an actively deforming foreland basin with up to 1-2 mm/yr differential subsidence. Note the prominent anticline and high-angle faulting in this region.